TRANSPORT PROBLEMS 2025 Volume 20 Issue 2
PROBLEMY TRANSPORTU DOI: 10.20858/tp.2025.20.2.12

Keywords: frontal collision; airbag control; vehicle occupants

Dominik GALDYNSKI[1*], Karol F. ABRAMEK[2], Wawrzyniec GOLEBIEWSKI[3], Tomasz OSIPOWICZ[4], Renata DOBRZYŃSKA[5]

MODIFICATION OF THE METHOD FOR DETERMINING HEAD-TO-AIRBAG CONTACT TIME DURING A VEHICLE COLLISION

Summary. This article presents a modified method for determining the activation timing of airbags in vehicles, which incorporates the real-time position of the driver's and passengers' heads. The primary objective of this modification is to improve the precision of airbag deployment by introducing an additional parameter—namely, the actual head position of the vehicle occupants, monitored in real time. The use of cameras and advanced image processing algorithms enables continuous tracking of head positions. As a result, the airbag system can adjust its activation timing according to the current positions of the occupants during a collision, significantly enhancing protective effectiveness. The results show that reducing the distance of the head from the normalized position by 70 mm requires the airbag activation to be advanced by an average of 28%. The largest correction occurs at a speed of 23 km/h and reaches 30%, decreasing at higher speeds. Conversely, increasing the distance by 70 mm necessitates the activation to be delayed by an average of 22%, with a maximum correction of 23% also observed at 23 km/h. These differences arise from the variable deceleration profile during a crash, which is influenced by specific collision dynamics. Unlike the conventional "13-30" model, which assumes a fixed head-to-airbag distance, the new method accounts for actual variations in occupant positioning, thereby improving protective performance. The proposed system uses infrared cameras and a lidar unit to track reference points on the head, such as the center of the forehead and the chin. Based on the collected data, the system dynamically adjusts the airbag deployment timing, reducing the risk of head injuries. This method can be integrated with other safety systems, such as seatbelt pretensioners and adaptive headrests, and is particularly applicable in autonomous vehicles, for which occupant positions may deviate significantly from standard seating postures. Adaptive airbag deployment has the potential to become a new standard in enhancing road safety.

1. INTRODUCTION

The airbag is the final significant step in vehicle passenger safety design, complementing seat belts. Despite its clear advantages, it can also pose risks. The first risk stems from excessively high inflation

[1] West Pomeranian University of Technology in Szczecin, Department of Automotive Engineering; Piastow av. 19, 70-310 Szczecin, Poland; e-mail: dgaldynski@zut.edu.pl; https://orcid.org/0000-0003-3232-2656
[2] West Pomeranian University of Technology in Szczecin, Department of Automotive Engineering; Piastow av. 19, 70-310 Szczecin, Poland; e-mail: kabramek@zut.edu.pl; https://orcid.org/0000-0001-9704-5253
[3] West Pomeranian University of Technology in Szczecin, Department of Automotive Engineering; Piastow av. 19, 70-310 Szczecin, Poland; e-mail: wgolebiewski@zut.edu.pl; https://orcid.org/0000-0002-3691-8636
[4] West Pomeranian University of Technology in Szczecin, Department of Automotive Engineering; Piastow av. 19, 70-310 Szczecin, Poland; e-mail: tosipowicz@zut.edu.pl; https://orcid.org/0000-0002-3321-7754
[5] West Pomeranian University of Technology in Szczecin, Department of Thermal Technologies and Safety Engineering; Piastów av. 41, 71-065 Szczecin, Poland; e-mail: renata.dobrzynska@zut.edu.pl; https://orcid.org/0000-0001-5469-5045
* Corresponding author. E-mail: dgaldynski@zut.edu.pl

pressure [20]. The second arises from the improper positioning of the driver and passenger [21]. The third comes from changes in vehicle body stiffness [3, 5]. The present study is focused on the second case.

Airbag activation is based on the analysis of the deceleration signal, recorded by an accelerometer located in the control module [8]. The magnitude of deceleration depends on the collision speed [4]. For different vehicle collision speeds, the activation time and, consequently, the airbag's reference state vary. Since the pressure development in the airbag follows a phased pattern, the contact between the head and the airbag must occur when the pressure inside the airbag has already reached its peak, but not later [17]. This point in the phased pressure curve allows for the optimal deceleration of the head and defines the timing for the airbag's maximum effectiveness.

During the design of the supplemental restraint system (SRS) at the vehicle development stage, the designated time for proper contact between the airbag and the driver's head is used to calibrate the airbag activation in such a way that it achieves its full functionality within this specified time. Due to the different structural designs of the vehicle body, as well as the materials and solutions used in the safety system itself, the system is developed individually for each vehicle.

The proper contact time between the driver's head and the airbag is determined based on the "13-30" rule [2, 6]. Using the deceleration profile recorded during a crash test for a selected collision speed, the head trajectory of the dummy and the vehicle are calculated. Taking into account the standardized positioning of the dummy's head and the vehicle's structural parameters, the time required for the airbag to reach full functionality is determined for a given distance, for example, '13 cm,' to properly engage the driver's head during a collision. The timing is similarly determined for other tested collision speeds.

The driver's position, as considered during the system's design, is crucial to maintain proper synchronization between the airbag deployment and the driver's head. A similar relationship applies to the passenger. The technical challenge associated with this assumption is that individuals of varying height, weight, or preferences will adopt different positions (distances) relative to the location of the airbag. Currently, airbag deployment is further adjusted using parameters collected from a passenger weight sensor installed in the seat structure and, in some cases, from a seat position sensor mounted on the adjustment rail. These sensors allow for an indirect estimation of the driver's or passenger's head position. However, such an interpretation is determined by assumptions about a standard (proper) seating position without accounting for positions that deviate from expected behavior. This raises questions about what happens when these assumptions are not met for the actual position of the driver or passenger. The head's position relative to the airbag can change, for instance, if the head is too close to or too far from the steering wheel or dashboard or if the person assumes an unusual posture that does not align with the seat's settings, such as torso rotation or leaning. The complexity increases when considering the impact of these variations on different body types and seating preferences. For example, shorter drivers might sit closer to the steering wheel, while taller passengers may need to recline their seats. Such differences highlight the need for more advanced adaptive systems that can dynamically adjust to the occupant's actual position in real-time.

In each of these cases, the position of the head relative to the airbag changes, and consequently, so does the distance the head travels during a collision before making contact with the deploying airbag. This means that the design assumptions regarding head position in the SRS for such scenarios would be incorrect.

2. CURRENT STATE OF KNOWLEDGE

The analysis of literature and patent applications reveals that the issue of modifying the airbag activation timing, considering the head position parameter, is currently in the conceptual stage among vehicle manufacturers. Therefore, an analysis initially based on the content of patent applications for inventions was conducted, followed by a review of articles.

In a patent [12], Toyota Motor specifies a method for using facial recognition and its position based on a camera image to control the timing of airbag deployment. In BMW AG's invention [13], an airbag control method was developed by which a camera image is used to identify the vehicle's interior, including head position recognition. In Honda Motor's invention [14], a device equipped with a camera that recognizes the head position of the person inside the vehicle was patented. Meanwhile, Ford [15] patented a method for controlling airbag deployment using an image from a camera mounted inside the vehicle. In another patent [16], Hyundai Motor Company outlines the possibility of controlling the airbag's opening angle, pressure, or inflation speed using a camera image.

In article [7], the authors describe an integrated, real-time passenger classification and tracking system based on vision technology using a single monochromatic camera. Article [18] discusses systems based on stereoscopic technology and long-wave infrared for "intelligent" airbag deployment. In article [1] from 2020, the authors present a model-based method for characterizing vehicle passengers using a 3D depth camera, which automatically estimates standard anthropometric data such as height, weight, and body shape by fitting a statistical body shape model to the depth image data.

The referenced articles highlight the dynamic development of vision technologies that are primarily used to detect the presence and distance of a passenger's face from the airbag to deactivate the airbag during a collision in the case of improper positioning. However, topics related to this article's focus are largely absent in these studies. The analysis of airbag activation timing modification systems, based on patent applications, revealed a lack of solutions for modifying the information about head position processed by the controller. This article proposes such a solution.

3. METHOD FOR MODIFYING THE PROCEDURE OF DETERMINING AIRBAG DEPLOYMENT TIME

The proposed solution is based on modifying the conventional method for determining airbag deployment timing by incorporating an additional parameter: the position of the driver's and passenger's heads. By using appropriate sensors (cameras), the system can dynamically adjust the airbag deployment timing to the actual head position at the moment of collision. This approach allows the standard time value—which was previously determined by the conventional "13-30" method—to be corrected by factoring in the real-time head position.

The analysis includes results presented in the example [11] using the following test parameters:

- Crash test standard: NHTSA FMVSS No. 208, frontal collision into a rigid barrier.
- Vehicle: Honda Civic.
- Collision speeds: 23, 32, 40, 48, and 56 km/h.
- Dummy: Driver without a fastened seatbelt.

The conventional "13-30" method estimates the airbag-to-head contact time for a standardized head position. This contact time is determined using empirically derived data from crash tests. The measurements of the dummy's head delay and vehicle deceleration in the steering wheel area are converted to establish the trajectory of their movement.

The difference in the coordinates of their trajectories for a given normative distance (e.g., "13 cm") can be expressed as $[S_b = f(t)] - [S_a = f(t)]$. This equation defines the time at which the airbag should achieve its full functionality. A graphical representation of this principle is shown in Fig. 2.

Similarly, the reference activation times of the airbag are determined for the other specified collision speeds.

Data source: NHTSA National Highway Traffic Safety Administration - NHTSA vehicle Crash Test Database, U. S. Department of Transportation [11].

A graphical representation of the empirically determined reference state times of the driver's airbag, with the driver wearing a seatbelt, based on five collision speeds, is shown in Fig. 3.

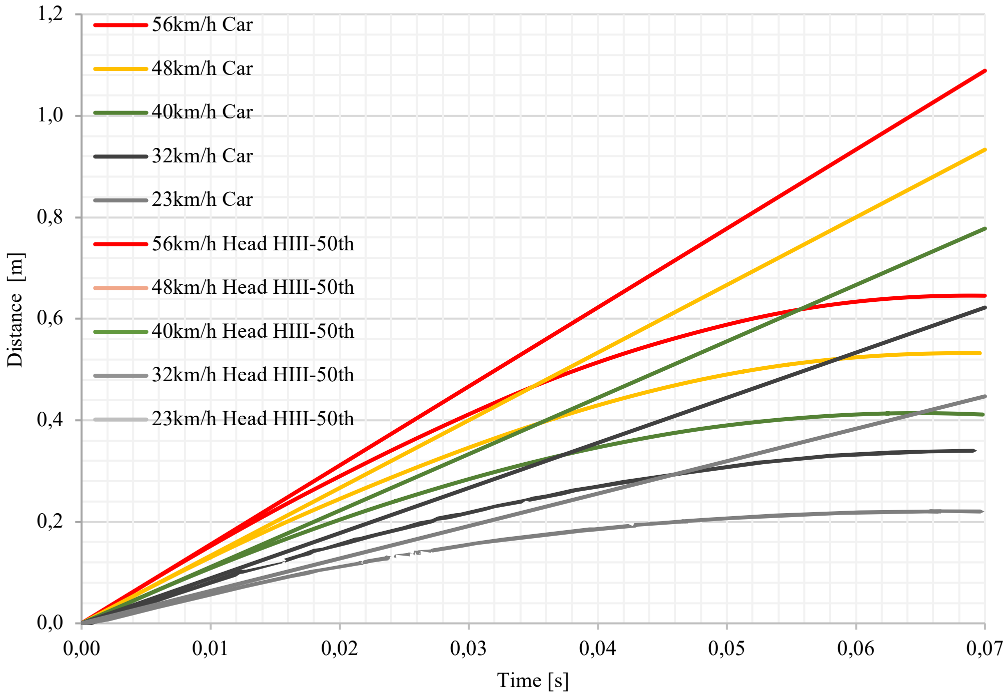

Fig. 1. Trajectory for the vehicle and head of an unbelted dummy over time at five collision speeds [11]

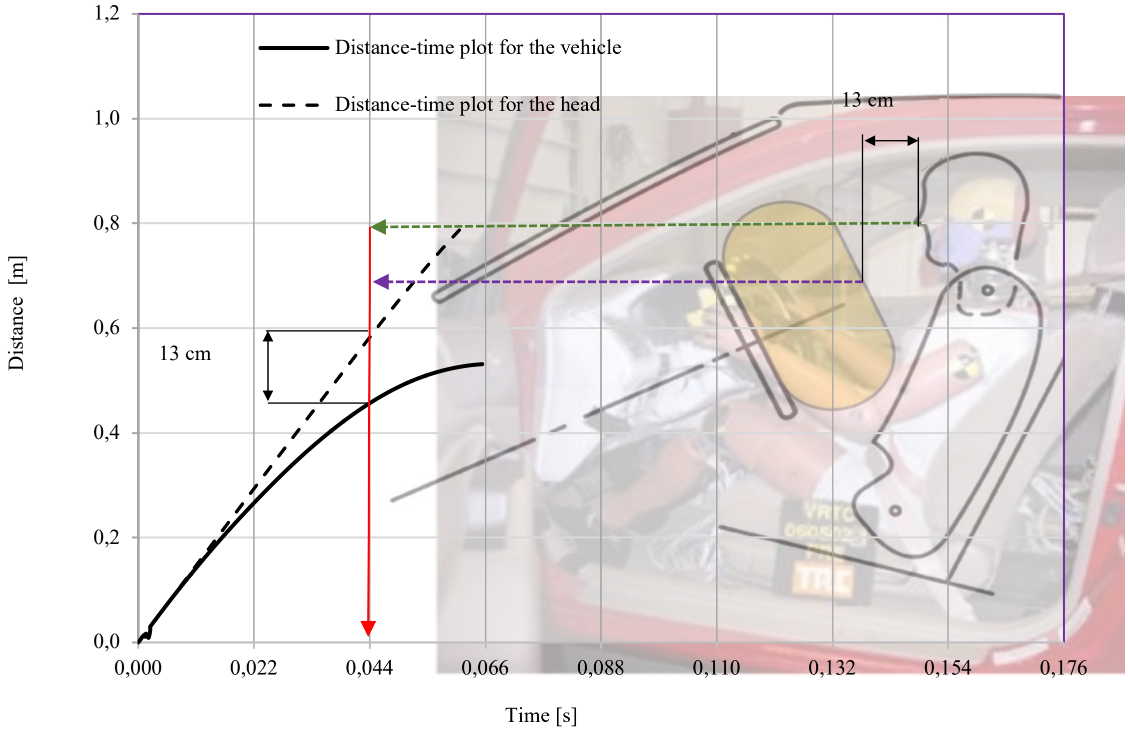

Fig. 2. Distance-time graph for the driver's head and the vehicle, with the indicated contact time of 0.044[s], at which the airbag should reach full functionality according to FMVSS208 crash test requirements at a speed of 48 km/h [11]

Table 1
Compilation of reference activation times for airbags for the HIII 50th percentile dummy, determined according to the "13-30" principle in a crash test with an unbelted dummy

Dummy/Vehicle Type: HIII 50th - Male, height 175 cm, weight 78 kg / Honda Civic	
Collision speed [km/h]	Reference airbag deployment status according to the "13-30" principle, without seatbelt usage [s]
56	0.043
48	0.044
40	0.046
32	0.049
23	0.054

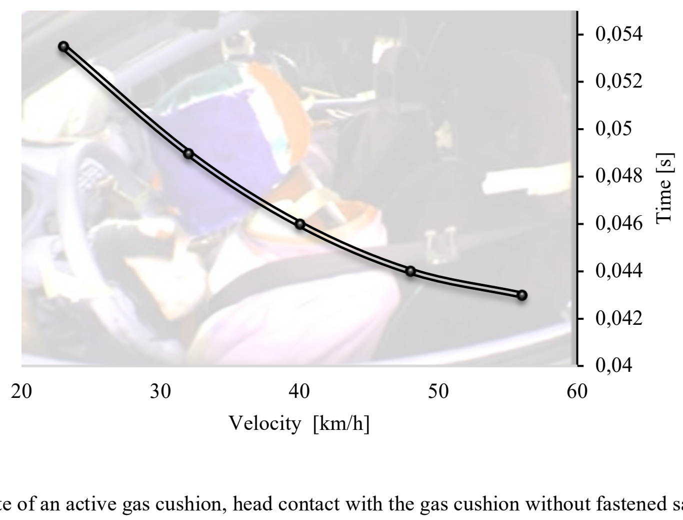

Fig. 3. Graphical relationship between the reference airbag deployment time for an unbelted driver and collision speed

Fig. 4 shows the recorded deceleration of the vehicle and the dummy's head during a crash test at a speed of 48 km/h. The noticeable shift from horizontal to vertical in the dummy's head deceleration at 44 ms indicates contact with the airbag.

The components of the time during which the SRS's actuators for frontal airbags are engaged can be divided into $T^K \wedge T^W \wedge T^D \wedge T^L \wedge T^A \wedge T^I = T'$,
where:
T^K – collision time [0 ms];
T^W – SRS system activation time /1 [g] ≈ 0.7-1.5 [ms], depending on speed;
T^D – diagnostics time [5 ms];
T^L – delay time in airbag activation /dependent on collision speed;
T^A – airbag activation time;
T^I – airbag inflation time;
T' – reference state time /head-to-airbag contact time.

In the modified method, the constant distance between the driver's head and the airbag for the standardized dummy position (e.g., "13 cm") is represented by the variable N_n. A graphical representation of this concept is shown in Fig. 3.

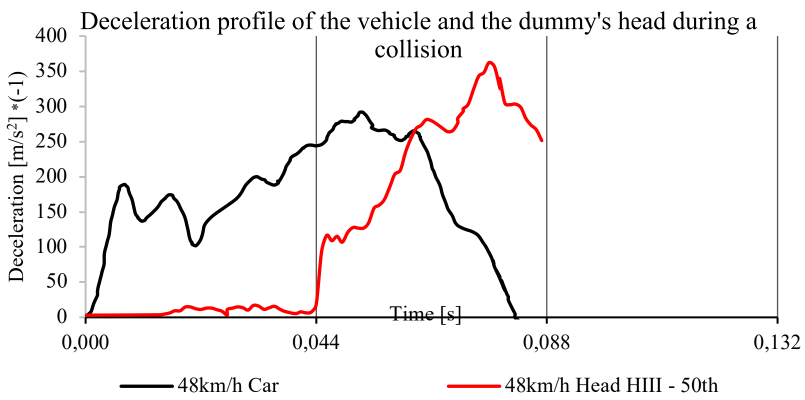

Fig. 4. Deceleration graph recorded for the vehicle and dummy's head during the FMVSS No. 208 crash test at a speed of 48 km/h, Honda Civic [11]

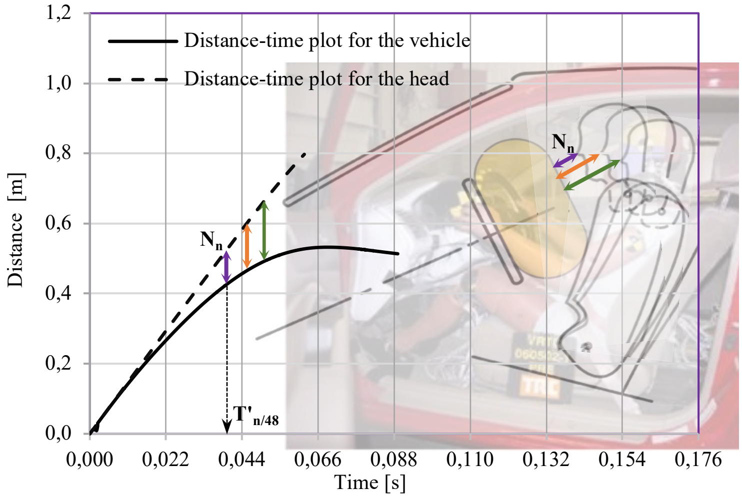

Fig. 5. Graph of distance-time between the driver's head and the vehicle, indicating the correct contact time at which the airbag should reach full functionality, depending on the driver's head position, based on the FMVSS 208 crash test at a speed of 48 km/h. The labels in the figure are explained in the text below

By calculating this difference, the system can determine the optimal deployment time for the airbag to fully inflate, ensuring maximum protection based on the head's specific position during impact. This method allows for precise timing adjustments that take into account individual variations in head position at the moment of impact. This adjustment allows for real-time adaptation of the airbag activation timing based on the actual head position of the driver or passenger.

Based on the collected data, for each pair of graphs (Fig. 1), the displacement parameters are determined as a function of time. From the difference in their $N_n = [S_b = f(t)] - [S_a = f(t)]$ coordinates, the time T'_n (Fig. 5) is calculated, at which the airbag should reach its full functionality (i.e., it should be fully deployed) for each possible N_n distance.

By introducing N, the system can dynamically modify the deployment time, ensuring that the airbag reaches its full protective capacity when the head is in a non-standard position during a collision. This enhances the vehicle's overall safety by accounting for variations in head position, which are not considered in the conventional "13–30" method. The reference state time of the airbag is determined analogously to the conventional method, with the value $N_n \in R$ representing a real-valued parameter that adjusts the timing. In this way, the time at which the airbag should achieve its full functionality is based on the actual distance of the driver's head at the moment of collision. The results obtained in this manner are arranged in a matrix, which takes the form of a Cartesian product N × V, where the set N represents defined head distances and the set V represents defined collision speeds. The value at their intersection, T′, determines the precise moment at which the head should make contact with the airbag to ensure full synchronization.

The analytical determination of the airbag deployment time, considering the actual distance between the head and the airbag and the collision speed, was carried out as follows.

For each collision speed, within the range of crash tests conducted—$V_n \in (V_{23}\ V_{32}\ V_{40}\ V_{48}\ V_{56}$—the interval of distance **N** ∈ R (X Y Z) was determined for the time range.

Based on these parameters, for each speed $V_n \in (V_{23}\ V_{32}\ V_{40}\ V_{48}\ V_{56})$, function graphs: $T'_{23}=f(N_{23})$; $T'_{30}=f(N_{30})$; $T'_{40}=f(N_{40})$; $T'_{48}=f(N_{40})$; $T'_{56}=f(N_{56})$, graphs of the following functions were plotted: $T'_{23}=f(N_{23})$; $T'_{30}=f(N_{30})$; $T'_{40}=f(N_{40})$; $T'_{48}=f(N_{40})$; $T'_{56}=f(N_{56})$

Using these determined functions and substituting the variable N_n, the results of the parameters were compiled in matrix form for the five speeds $V_{23/32/40/48/56}$

Table 2

Matrix of head-to-airbag contact times $T'_{n/V}$
for selected collision speeds (V_{23}, V_{32}, V_{40}, V_{48}, V_{56}) and head distances (N_1, N_2, ..., N_n)

	V_{23}	V_{32}	V_{40}	V_{48}	V_{56}
N_1	$T'_{1/23}=f(N_1)$	$T'_{1/32}=f(N_1)$	$T'_{1/40}=f(N_1)$	$T'_{1/48}=f(N_1)$	$T'_{1/56}=f(N_1)$
N_2	$T'_{2/23}=f(N_2)$	$T'_{2/32}=f(N_2)$	$T'_{2/40}=f(N_2)$	$T'_{2/48}=f(N_2)$	$T'_{2/56}=f(N_2)$
N_3	$T'_{3/23}=f(N_3)$	$T'_{3/32}=f(N_3)$	$T'_{3/40}=f(N_3)$	$T'_{3/48}=f(N_3)$	$T'_{3/56}=f(N_3)$
….	…..	…..	…..	……	…...
N_n	$T'_{n/23}=f(N_n)$	$T'_{n/32}=f(N_n)$	$T'_{n/40}=f(N_n)$	$T'_{n/48}=f(N_n)$	$T'_{n/56}=f(N_n)$
N_{n+1}	$T'_{n+1/23}=f(N_{n+1})$	$T'_{n+1/32}=f(N_{n+1})$	$T'_{n+1/40}=f(N_{n+1})$	$T'_{n+1/48}=f(N_{n+1})$	$T'_{n+1/56}=f(N_{n+1})$

Additional graphs were generated using the data formed from the coordinates of these graphs, recorded in matrix form; these were described by the function $T'=f(V_m)$. Based on these functions, for each of the analyzed speeds V_m, the value of T' was determined from the coordinates of these graphs and presented in the form of a Cartesian product matrix N x V.

Table 3

Matrix of head-to-airbag contact time functions $T'_{n/V}$
for various head distances (N_1, N_2, ..., N_n) and collision speeds (V_{23}, V_{24}, ..., V_m, $V_{(m+1)}$)

	V_{23}	V_{24}	…..	V_m	V_{m+1}
N_1	$T'_{1/23}=f(V_{23})$	$T'_{1/24}=f(V_{24})$	……	$T'_{1/m}=f(V_m)$	$T'_{1/48}=f(V_{m+1})$
N_2	$T'_{2/23}=f(V_{23})$	$T'_{2/24}=f(V_{24})$	….	$T'_{2/m}=f(V_m)$	$T'_{2/48}=f(V_{m+1})$
N_3	$T'_{3/23}=f(V_{23})$	$T'_{3/24}=f(V_{24})$	…..	$T'_{3/m}=f(V_m)$	$T'_{3/48}=f(V_{m+1})$
……	……….	………..	…..	………..	……….
N_n	$T'_{n/23}=f(V_{23})$	$T'_{n/24}=f(V_{24})$	…..	$T'_{n/m}=f(V_m)$	$T'_{n/48}=f(V_{m+1})$
N_{n+1}	$T'_{n+1/23}=f(V_{23})$	$T'_{n+1/24}=f(V_{24})$	…….	$T'_{n+1/m}=f(V_m)$	$T'_{n+1/48}=f(V_{m+1})$

The determined matrix elements enable the control module of the SRS to identify the correct head-to-airbag contact time for a given collision speed and distance measured by the camera, ensuring proper synchronization.

Tables 4 and 5 in the appendix present the calculation results for speeds V from 23 to 56 [km/h] and distances N from 0.06 to 0.23 [m]. The coordinate parameters form data that, when stored in matrix form within the SRS controller, determine the airbag deployment time for a given collision speed.

4. OPTICAL HEAD POSITION MONITORING SYSTEM

A thermal camera system with a wide-angle lens operates in conjunction with real-time image analysis software. This enables the driver's head position to be tracked in a three-dimensional space, allowing the dynamic adjustment of the front airbag parameters, thereby enhancing safety in the event of a collision. The system utilizes advanced image analysis algorithms that can recognize key anatomical landmarks on the driver's face and head, such as the center of the forehead, chin, and nose. By monitoring the changes in the position of these points over time, the system calculates the distance of the head from the steering wheel and its tilt. This is crucial for precisely adjusting the airbag's deployment timing based on the driver's head position [9].

The driver's head position monitoring system integrates two key technologies: thermal cameras and light detection and ranging (lidar). Thermal cameras operate in the infrared spectrum, making them independent of lighting conditions inside the vehicle. Additionally, the camera is equipped with a wide-angle lens, allowing it to monitor a large area that includes both the driver and adjacent passengers. This setup enables the rapid detection of changes in body or head posture [9].

Lidar complements the monitoring system by providing precise mapping of the three-dimensional space inside the vehicle cabin. Thanks to lidar, the system can generate a 3D map of the vehicle interior and accurately determine the distance of the driver's head from the steering wheel, as well as detect real-time positional changes. This technology improves the accuracy of analysis and reduces measurement errors caused by image processing delays and varying lighting conditions [10]. The variety of solutions for the placement of head position monitoring devices in a vehicle is specific to each manufacturer [12-16].

The architecture of this system consists of the following components:

- **Thermal camera:** Mounted on the dashboard, it collects data in the form of heat maps, which are processed by image analysis algorithms.
- **Lidar:** Provides accurate mapping of the vehicle's interior, enabling the identification of the head position and other objects within the cabin.
- **Image analysis software:** Utilizes deep learning algorithms to identify anatomical points on the face and track head movements.
- **Airbag control module:** Receives signals from the image analysis software and adjusts the airbag deployment timing based on head position.

A crucial component of the image analysis algorithm is the detection of facial landmarks, such as the eyes, nose, chin, and forehead edges. Neural networks based on deep learning are used to recognize these points with high accuracy, even under varying lighting conditions. To effectively monitor the driver's head position, the system employs the following algorithm:

- **Input:** Images from the thermal camera and data from lidar.
- **Pre-processing:** Noise removal and image smoothing.
- **Facial landmark detection:** Utilizes a neural network to recognize key points such as eyes, nose, mouth, and facial contours.
- **Head movement tracking:** Analyzes the trajectory of key points in real time to calculate the distance from the steering wheel and the head's tilt angle.
- **Airbag parameter adjustment:** Based on the head position, the algorithm adjusts the airbag deployment timing to minimize the risk of injury.

5. CONCLUSIONS

The primary goal of modifying the traditional method was to increase the precision of the airbag activation moment by introducing a new parameter—namely, the real-time position of the driver's head. This change ensures optimal airbag deployment in the event of head contact during a collision. The modification enables the dynamic adjustment of activation timing, allowing the value derived from traditional methods to be corrected based on the current head distance. As a result, the airbag activation time can be set with greater accuracy.

The analysis of the results presented in Tables 4 and 5 demonstrates that reducing the distance from the standardized position of the driver's dummy head by 70 mm relative to the front airbag requires the activation timing to be accelerated by an average of 28%. The highest adjustment in activation timing is required at a speed of 23 km/h, accounting for 30%, and decreases as the speed increases.

Meanwhile, increasing the distance from the standardized head position by 70 mm requires the activation time to be delayed by an average of 22%. The highest correction is required at 23 km/h, amounting to 23%, and decreases as speed increases. The observed difference in the average results between accelerating and delaying airbag activation arises from the variable nature of deceleration during a collision.

Fig. 6 is a graphical representation of the percentage adjustment of the airbag activation timing, depending on the change in the head distance of the driver dummy relative to the normalized position and collision speed.

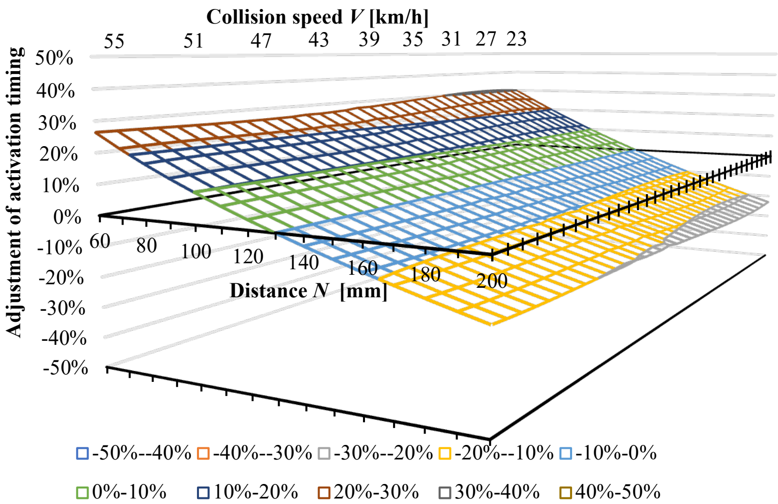

Fig. 6. Graphical representation of the percentage adjustment of the airbag activation timing based on changes in the head distance of the driver dummy relative to the normalized position and collision speed

Integrating the new parameter—the actual head distance—enables the airbag system to respond to changes in real time. That is, the airbag will activate not only based on collision speed but also in a way that adapts to the passenger's actual position at the moment of impact. This approach aligns with modern trends in active vehicle safety systems, by which adaptability and real-time response are crucial to minimizing injury severity.

Potential Benefits and Broader Applications

- **Enhanced passenger protection**: A direct effect of this method is a significant reduction in head injuries, especially in scenarios where the head position deviates from standard settings. In this way, the method increases the reliability of the airbag's performance and reduces the risk that airbags will cause injury.
- **Integration with other vehicle systems**: This method can be integrated with existing driver assistance systems, such as seatbelt pretensioners, adaptive headrests, or fatigue monitoring systems. As vehicle safety technology evolves, this methodology can be extended to side airbags and curtains, for which head position plays a crucial role.
- **Future innovations**: With the increasing popularity of autonomous and semi-autonomous systems, passenger positions will become increasingly varied, making adaptive safety systems even more important.
- **Broader safety standards**: This approach could establish new regulatory standards for future airbag systems, requiring them to consider dynamic passenger positioning. This would contribute to overall safety improvements in the automotive industry across all market segments.

References

1. Byoung-Keon Park, D.J. & Kozak, K. & Reed, M.P. Model-based characterisation of vehicle occupants using a depth camera. *International Journal of Vehicle Design*. 2020. P. 23-37. DOI: 10.1504/IJVD.2020.114780.

2. Ching-Yao, Ch. *Fundamentals of Crash Sensing in Automotive Air Bag Systems*. Published by SAE International. 2000. ISBN: 9780768063783.
3. Hadrys, D. & Kubik, A. & Stanik, Z. Deceleration and deformation during dynamic loading of model car body parts after post-accident repair. *Transport Problems.* 2020. Vol. 15. No. 3. P. 5-16.
4. Hannan, M.A. & Hussai, A. & Mohamed, A. et al. Decision fusion of a multi-sensing embedded system for occupant safety measures. *International Journal of Automotive Technology*. 2010. Vol. 11. No. 1. P. 57-65.
5. Gałdynski, D. & Abramek, K.F. & Lisowski, M. et al. Heuristic model for assessing disruptions in the synchronization of airbag deployment with the driver's body during a collision, based on repaired longitudinal beams. *Transport Problems.* 2024. Vol. 19 No. 1. P. 131-142.
6. International Motor Vehicle Inspection Committee Raport 8328. *A Test Procedure for Airbags*. Institut für Kraftfahrwesen Aachen. 2000.
7. Jain, A.K. & Farmer, M.E. Smart automotive airbags: Occupant classification and tracking. *IEEE Transactions on Vehicular Technology*. 2007. P. 60-80.
8. Kamiński, T. & Niezgoda, M. & Kruszewski, M. Collision detection algorithms in the ecall system. *Journal of KONES Powertrain and Transport*. 2012. Vol. 19. No. 4. P. 267-274.
9. Kirmas, A. & Lemcke, S. & Böshagen, S. et al. Head tracking in automotive environments for driver monitoring using a low resolution thermal camera. *Vehicles.* 2022. No. 4. P. 219-233.
10. Mishra, A. & Lee, S. & Kim, D. & Kim, S. In-cabin monitoring system for autonomous vehicles. *Sensors* 2022. Vol. 22. No. 4360.
11. NHTSA VSR - *NHTSA Vehicle Crash Test Database*. No. crashtest: TC 03-228 RR04-232, Tc 03-229 RR04-221, DTS-TRC-03-005, 030806-1, 060502-1, NCAP-MGA-2001-004). Available at: https://www-nrd.nhtsa.dot.gov/database/veh/veh.htm.
12. Patent JP2010100142. *Vehicular Device Control Device.* Toyota Motor Corp, Japan. (Uozumi, S.) Publ. 06.05.2010.
13. Patent DE10308405. *Airbag Control Method for Motor Vehicle, Uses Camera to Determine Actual Position of Vehicle Occupant's Head with Respect to Preset Position to Control Airbag Ignition.* Bayerische Motoren Werke AG, Germany. (Augst, A. & Borke, D. & Durach, S.) Publ. 27.02.2003.
14. Patent JP2006290258. *Occupant Restraining Device.* Honda Motor Co Ltd, Japan. (Takemura, N.) Publ. 13.04.2005.
15. Patent CN110395208. *Control the air bag activation state at motor vehicles.* Ford Global Technologies LLC. Chinese. Publ. 01.11.2019.
16. Patent US10131309. *Apparatus and method for controlling airbag.* Hyundai Motor Co. US. (Seon, A. K.) Publ. 20.11.2018.
17. Rastegar, V. & Marzbanrad, J. Modeling and simulation of vehicle airbag behaviour in crash. *International Scientific Journal "Industry 4.0"*. 2018. Vol. 3. P. 126-129.
18. Trivedi, M.M. & Krotosky, S.J. & Cheng, S.Y. Face detection and head tracking using stereo and thermal infrared cameras for "smart" airbags: a comparative analysis. *Proceedings The 7th International IEEE Conference on Intelligent Transportation Systems.* 2004. P. 17-22.
19. Wang, X. & Luo, Z. & Liu, Y. & Ling F. Fatigue properties of advanced high strength steel plate welded by hybrid plasma arc welding. *Procedia Structural Integrity*. 2019. Vol. 22. P. 59-63.
20. Winch, M. & Hollowell, T.W. & Kanianthra, J. & Evans, W.D. *Air Bag Technology in light passenger vehicles*. Office of Research and Development National Highway Traffic Safety Administration. USA. 2001.
21. Vangi, D. *Vehicle Collision Dynamics, Analysis and Reconstruction*. Department of Industrial Engineering, University of Florence. Italy. 2020.

Received 01.11.2023; accepted in revised form 09.06.2025

Appendix

Table 4

Matrix of head-to-airbag contact time functions $T'_{n/V}$
for various head distances N from 0.06 to 0.14 [m] and collision speeds (V_{23}, V_{24}, ..., V_{56})

Collision speed [km/h]	Head distance [m]								
	0.06	***0.07***	***0.08***	***0.09***	***0.10***	***0.11***	***0.12***	***0.13***	***0.14***
23	0.037	0.040	0.043	0.045	0.047	0.049	0.051	**0.054**	0.055
24	0.037	0.039	0.042	0.044	0.047	0.049	0.051	0.053	0.055
25	0.036	0.039	0.041	0.044	0.046	0.048	0.050	0.053	0.055
26	0.036	0.038	0.041	0.043	0.046	0.048	0.050	0.052	0.054
27	0.036	0.038	0.040	0.043	0.045	0.047	0.049	0.051	0.053
28	0.035	0.038	0.040	0.042	0.045	0.047	0.049	0.051	0.053
29	0.035	0.037	0.040	0.042	0.044	0.046	0.048	0.050	0.052
30	0.035	0.037	0.039	0.041	0.044	0.046	0.048	0.050	0.052
31	0.034	0.037	0.039	0.041	0.043	0.045	0.047	0.049	0.051
32	0.034	0.036	0.039	0.041	0.043	0.045	0.047	**0.049**	0.050
33	0.034	0.036	0.038	0.040	0.042	0.044	0.046	0.048	0.050
34	0.034	0.036	0.038	0.040	0.042	0.044	0.046	0.048	0.049
35	0.034	0.036	0.038	0.040	0.042	0.044	0.045	0.047	0.049
36	0.033	0.036	0.038	0.040	0.041	0.043	0.045	0.047	0.048
37	0.033	0.035	0.037	0.039	0.041	0.043	0.045	0.046	0.048
38	0.033	0.035	0.037	0.039	0.041	0.043	0.044	0.046	0.048
39	0.033	0.035	0.037	0.039	0.041	0.042	0.044	0.046	0.047
40	0.033	0.035	0.037	0.039	0.040	0.042	0.044	**0.046**	0.047
41	0.033	0.035	0.037	0.039	0.040	0.042	0.043	0.045	0.046
42	0.033	0.035	0.037	0.038	0.040	0.042	0.043	0.045	0.046
43	0.033	0.035	0.037	0.038	0.040	0.042	0.043	0.045	0.046
44	0.033	0.035	0.036	0.038	0.040	0.041	0.043	0.045	0.046
45	0.033	0.035	0.036	0.038	0.040	0.041	0.043	0.044	0.046
46	0.033	0.034	0.036	0.038	0.040	0.041	0.043	0.044	0.045
47	0.033	0.034	0.036	0.038	0.039	0.041	0.043	0.044	0.045
48	0.033	0.034	0.036	0.038	0.039	0.041	0.042	**0.044**	0.045
49	0.032	0.034	0.036	0.038	0.039	0.041	0.042	0.044	0.045
50	0.032	0.034	0.036	0.038	0.039	0.041	0.042	0.044	0.045
51	0.032	0.034	0.036	0.038	0.039	0.041	0.042	0.044	0.045
52	0.032	0.034	0.036	0.037	0.039	0.041	0.042	0.044	0.045
53	0.032	0.034	0.036	0.037	0.039	0.041	0.042	0.043	0.045
54	0.032	0.034	0.036	0.037	0.039	0.040	0.042	0.043	0.045
55	0.032	0.034	0.036	0.037	0.039	0.040	0.042	0.043	0.045
56	0.032	0.034	0.035	0.037	0.039	0.040	0.042	**0.043**	0.044

Table 5

Matrix of head-to-airbag contact time functions $T'_{n/V}$
for various head distances N from 0.15 to 0.23 [m] and collision speeds (V_{23}, V_{24}, ..., V_{56})

		Head distance [m]								
		0.15	***0.16***	***0.17***	***0.18***	***0.19***	***0.20***	***0.21***	***0.22***	***0.23***
Collision speed [km/h]	***23***	0.057	0.059	0.061	0.063	0.064	0.066	0.067	0.069	0.070
	24	0.057	0.059	0.061	0.062	0.064	0.065	0.067	0.068	0.070
	25	0.056	0.058	0.060	0.062	0.063	0.065	0.067	0.068	0.069
	26	0.056	0.058	0.060	0.061	0.063	0.064	0.066	0.067	0.069
	27	0.055	0.057	0.059	0.061	0.062	0.064	0.065	0.067	0.068
	28	0.055	0.057	0.058	0.060	0.062	0.063	0.065	0.066	0.067
	29	0.054	0.056	0.058	0.059	0.061	0.062	0.064	0.065	0.067
	30	0.054	0.055	0.057	0.059	0.060	0.062	0.063	0.064	0.066
	31	0.053	0.055	0.056	0.058	0.059	0.061	0.062	0.064	0.065
	32	0.052	0.054	0.056	0.057	0.059	0.060	0.061	0.063	0.064
	33	0.052	0.053	0.055	0.056	0.058	0.059	0.061	0.062	0.063
	34	0.051	0.053	0.054	0.056	0.057	0.059	0.060	0.061	0.062
	35	0.050	0.052	0.054	0.055	0.056	0.058	0.059	0.060	0.062
	36	0.050	0.052	0.053	0.054	0.056	0.057	0.058	0.060	0.061
	37	0.049	0.051	0.052	0.054	0.055	0.057	0.058	0.059	0.060
	38	0.049	0.050	0.052	0.053	0.055	0.056	0.057	0.058	0.060
	39	0.049	0.050	0.051	0.053	0.054	0.055	0.057	0.058	0.059
	40	0.048	0.050	0.051	0.052	0.054	0.055	0.056	0.057	0.058
	41	0.048	0.049	0.051	0.052	0.053	0.054	0.056	0.057	0.058
	42	0.048	0.049	0.050	0.052	0.053	0.054	0.055	0.056	0.058
	43	0.047	0.049	0.050	0.051	0.053	0.054	0.055	0.056	0.057
	44	0.047	0.048	0.050	0.051	0.052	0.053	0.055	0.056	0.057
	45	0.047	0.048	0.050	0.051	0.052	0.053	0.054	0.055	0.056
	46	0.047	0.048	0.049	0.051	0.052	0.053	0.054	0.055	0.056
	47	0.047	0.048	0.049	0.050	0.052	0.053	0.054	0.055	0.056
	48	0.047	0.048	0.049	0.050	0.052	0.053	0.054	0.055	0.056
	49	0.047	0.048	0.049	0.050	0.051	0.053	0.054	0.055	0.056
	50	0.046	0.048	0.049	0.050	0.051	0.052	0.053	0.054	0.055
	51	0.046	0.048	0.049	0.050	0.051	0.052	0.053	0.054	0.055
	52	0.046	0.048	0.049	0.050	0.051	0.052	0.053	0.054	0.055
	53	0.046	0.047	0.049	0.050	0.051	0.052	0.053	0.054	0.055
	54	0.046	0.047	0.048	0.050	0.051	0.052	0.053	0.054	0.055
	55	0.046	0.047	0.048	0.049	0.050	0.051	0.052	0.053	0.054
	56	0.046	0.047	0.048	0.049	0.050	0.051	0.052	0.053	0.054